High Resolution Solid-State NMR and DSC Study of Poly(ethylene glycol)-Silicate Hybrid Materials Via Sol–Gel Process

WEIBIN CHEN,[1] HANQIAO FENG,[1] DAYONG HE,[2] CHAOHUI YE[1]

[1] Laboratory of Magnetic Resonance and Atomic and Molecular Physics, Wuhan Institute of Physics and Mathematics, Chinese Academy of Sciences, Wuhan 430071, People's Republic of China

[2] Polymer Physics Laboratory, Changchun Institute of Applied Chemistry, Chinese Academy of Sciences, Changchun 130022, People's Republic of China

Received 3 April 1997; accepted 30 May 1997

ABSTRACT: Hybrid materials incorporating poly(ethylene glycol) (PEG) with tetraethoxysilane (TEOS) via a sol–gel process were studied for a wide range of compositions of PEG by DSC and high resolution solid-state ^{13}C- and ^{29}Si-NMR spectroscopy. The results indicate that the microstructure of the hybrid materials and the crystallization behavior of PEG in hybrids strongly depend on the relative content of PEG. With an increasing content of PEG, the microstructure of hybrid materials changes a lot, from intimate mixing to macrophase separation. It is found that the glass transition temperatures (T_g) (around 373 K) of PEG homogeneously embedded in a silica network are much higher than that (about 223 K) of pure PEG and also much higher in melting temperatures T_m (around 323 K) than PEG crystallites in heterogeneous hybrids. Meanwhile, the lower the PEG content, the more perfect the silica network, and the higher the T_g of PEG embedded in hybrids. An extended-chain structure of PEG was supposed to be responsible for the unusually high T_g of PEG. Homogeneous PEG-TEOS hybrids on a molecular level can be obtained provided that the PEG content in the hybrids is less than 30% by weight. © 1998 John Wiley & Sons, Inc. J Appl Polym Sci **67:** 139–147, 1998

Key words: PEG-TEOS hybrid materials; microstructure; mobility; solid-state ^{13}C- and ^{29}Si-NMR; DSC

INTRODUCTION

In recent years, study of hybrid materials, obtained through the sol–gel process by incorporating organic polymers with tetraethoxysilane or tetramethoxysilane (TEOS or TMOS),[1–6] has become popular as a simple and efficient approach to develop new organic–inorganic composite materials with special performance. By properly controlling the conditions of hydrolysis and condensation of TEOS in the presence of a preformed organic polymer, it is usually possible to obtain optically transparent composite materials in which organic polymers are homogeneously embedded within a 3-dimensional SiO_2 network.[1] It is found that the existence of special functional groups in the polymer, which may form hydrogen bonds with silanol groups or covalent bonds with the inorganic phases, is favorable for the formation of optically transparent materials.[1–3] In addition, factors such as the molecular weight of the polymer and the content of polymer in hybrids are also found to have a significant effect on the morphology of composite materials.[1,2]

In this work a typical polymer, poly(ethylene

Correspondence to: Prof. H. Feng.

Journal of Applied Polymer Science, Vol. 67, 139–147 (1998)
 CCC 0021-8995/98/010139-09

glycol) (PEG), was chosen as a preformed polymer to form a hybrid with TEOS because it has two features: it is crystallizable, and it has terminal hydroxyl groups that are expected to form hydrogen bonding with the silanol group and/or form C—O—Si covalent bonds with the silica network. The microstructure of PEG-TEOS hybrids, the mobility of PEG in the hybrids, and the crystallization behavior of PEG in the hybrids were systematically studied by DSC and solid-state NMR techniques. Some novel results were obtained.

EXPERIMENTAL

High purity TEOS was obtained from the Fluka Company of Japan without further purification. PEG (M_w = 2000) and tetrahydrofuran (THF, as solvent) were purified before use to insure homogeneous solutions.

A highly schematic mechanism for hydrolysis–condensation reactions for TEOS is shown below:

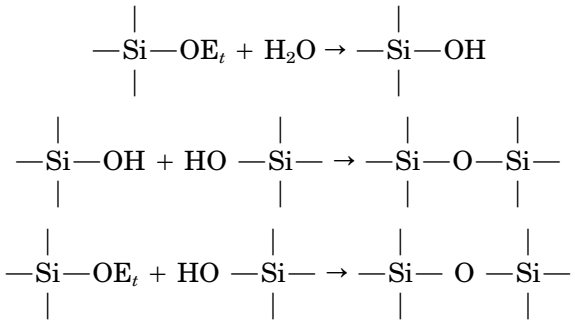

Ion-free water (1.6 mL) and hydrochloric acid (2M, 0.1 mL) were first added to a 100-mL round-bottom flask with 20 mL of THF, and the mixture was stirred thoroughly. Then TEOS (5 mL) and an appropriate amount of PEG were simultaneously added to the flask that was placed in an oil bath (338–343 K); the reaction took place under reflux with fast agitation for 0.5 h. After cooling, the clear liquid was poured into a Teflon-coated Petri dish and covered with parafilm to allow the system to gel. After 2 weeks at ambient all of the samples gelled and the parafilm was removed to continue the drying process at 323 K for 1 week. Specimens were further dried at 313 K under a vacuum for 2 weeks prior to measuring. The compositions of the initial reactive solutions and the appearance of final products are listed in Table I.

In this study, all the reaction conditions were kept constant except for the PEG content. The amount of water added to initiate the hydrolysis reaction was stoichiometric; the molar ratio of HCl to TEOS was 0.01 : 1. We found that the degree of transparency of the final hybrid materials strongly depended on the relative content of PEG. Specimens 2 and 3 had a lower content of PEG and were large pieces of transparent films; specimens 4, 5, and 6 had a middle content of PEG and were semitransparent and brittle; and specimens 7 and 8 had a higher content of PEG and were opaque. The appearance of these hybrids showed that their microstructures were quite different.

DSC experiments were performed on a Perkin–Elmer DSC-7. The following thermal procedure was used: heating from 280 to 520 K with a heating rate of 20 K/min, holding 5 min at 520 K, and cooling from 520 to 280 K with a cooling rate of −20 K/min. The hold at 520 K was used to avoid the effect of thermodynamic history. The crystallization temperature (T_{cr}) was determined as a maximum of the exothermic peak of crystallization. The heating run gave the melting temperature (T_m) as the maximum of the endothermic peak. The temperature at the midpoint of the heat capacity transition was taken as the glass transition temperature (T_g).

Solid-state cross polarization magic angle spinning (CPMAS) NMR experiments were performed on a Bruker MSL-400 NMR spectrometer at 298 K. The hydrogen resonance frequency was 400.13 MHz, and the ^{13}C resonance frequency was 100.63 MHz. A 5.5-μs 90° pulse for the ^{13}C nucleus and a 4.8-μs 90° pulse for ^{1}H were used. The contact time was 1.0 ms and the MAS rate was 4.0 kHz. ^{13}C spin-lattice relaxation times [T_1(C)] were measured by the CP T_1 method. [7] ^{1}H spin-lattice relaxation times in the rotating frame, $T_{1\rho}$(H), were obtained from the ^{13}C CPMAS intensity with increasing contact times. ^{13}C spectra were referred to the chemical shift of methyl group carbons of hexamethylbenzene, which is 16.9 ppm. ^{29}Si resonance frequency was 79.46 MHz, and the MAS rate was 1.5 kHz. ^{29}Si spectra were referred to the chemical shift of the methyl group silicons of tetrakis(trimethylsilyl)silane (TKS), which is −9.8 ppm.

RESULTS AND DISCUSSION

DSC Measurements

Shown in Figures 1 and 2 are the DSC traces for the selected samples 2, 3, 6, and 8: the corresponding thermal data are listed in Table II.

Table I Preparation Conditions of PEG-TEOS Hybrid Materials

Sample No.	TEOS (mL)	PEG (g)	H_2O (mL)	HCl (2*M*) (mL)	wt % SiO_2 in Final Product[a]	State
1	0	Pure PEG			0	
2	5	0.1	1.6	0.1	93.2	T
3	5	0.4	1.6	0.1	77.5	T
4	5	0.8	1.6	0.1	63.2	T/S
5	5	1.0	1.6	0.1	58.0	S
6	5	1.2	1.6	0.1	53.5	S
7	5	1.6	1.6	0.1	46.3	O
8	5	1.8	1.6	0.1	43.3	O

T, transparent; S, semitransparent; O, opaque.
[a] Assuming reaction is complete.

There are several features about the DSC results worthy of mention. The T_g values (353–373 K) of PEG in the hybrids are much higher than that of pure PEG (around 223 K)[8]; the lower the content of PEG, the higher the T_g of PEG in the hybrids. Hybridization has a dramatic effect on the crystallization behavior of PEG. Only when the content of PEG is more than some value (for example, 40% by weight in this case) can detectable PEG crystallites form. An unusual phenomenon observed is that the T_g of PEG in hybrids is much higher than its T_m. Meanwhile, it is also found that the higher the relative content of PEG in the hybrids, the lower the T_m and T_{cr} of PEG, and the larger the ΔH_f and ΔH_{cr} of PEG. When the content of PEG is big enough, such as in sample 8, the T_m of PEG crystallites in hybrids is the same as that of pure PEG,[9] implying that the PEG domain size is so big that the existence of the silica network has little effect on the crystallization behavior of PEG. The above DSC results indicate that the morphology of PEG chains in silica networks changes a lot with the increase in PEG content, from intimately mixing with the silica net-

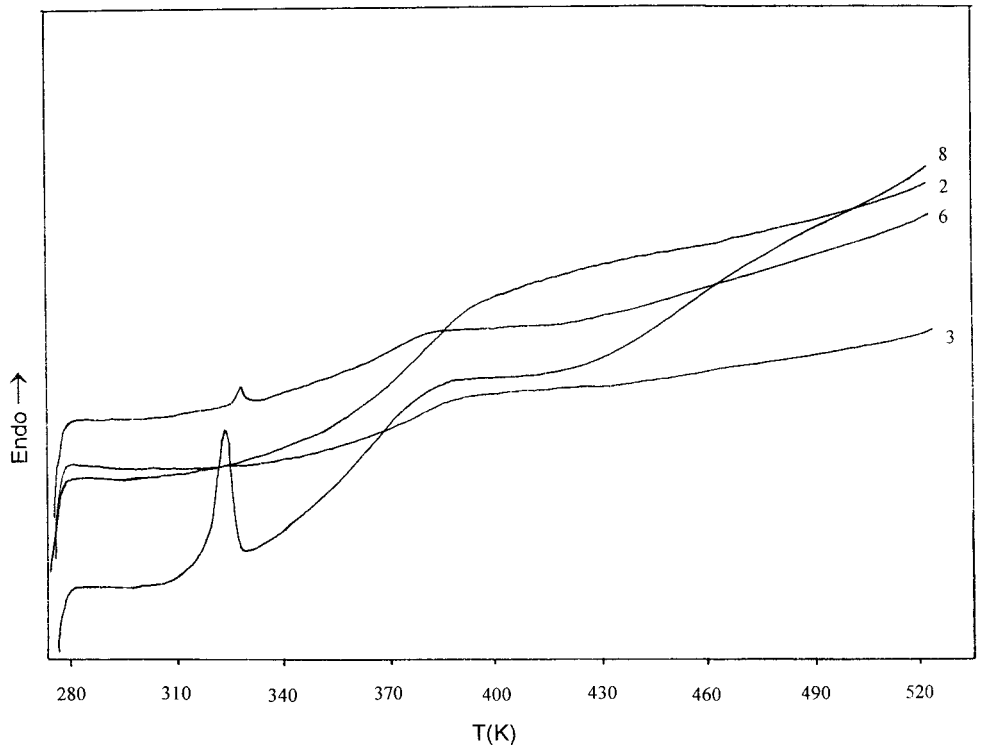

Figure 1 DSC melting curves for samples 2, 3, 6, and 8.

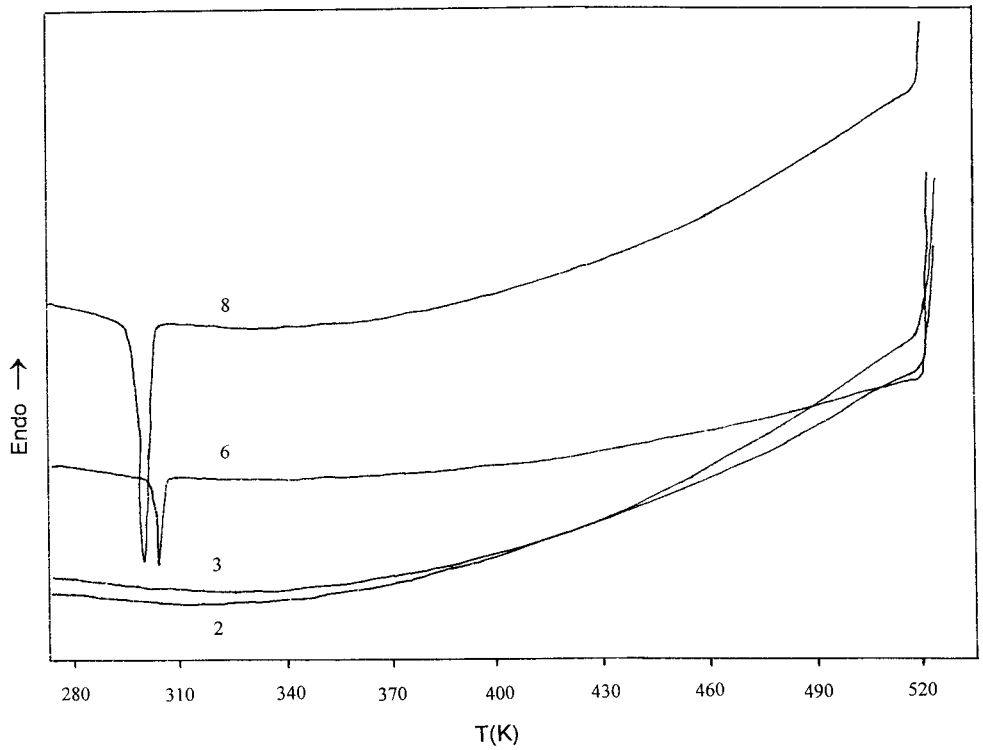

Figure 2 DSC crystallization curves for samples 2, 3, 6, and 8.

work to microphase separation, and finally to macrophase separation. For hybrids with lower PEG content (samples 2 and 3), it seems that PEG chains are embedded in the 3-dimensional silica networks. Therefore, the PEG has T_g values much higher than that of pure PEG and loses its crystallizability due to the restrictions imposed by the dense silica network. Meanwhile, the T_g values of PEG in hybrids, to some degree, decrease with increasing content of PEG. The possible reasons for this may be small domains rich in PEG tend to be formed with the increase in the PEG content, or the silica network becomes looser and looser with increasing PEG content. With a further increase in PEG content, the region rich in PEG becomes large enough for the formation of a small quantity of PEG crystallites. Sample 6 is an example of this kind of hybrid. Finally, macrophase separation occurs for the hybrid containing a much higher content of PEG like sample 8.

At first sight it seems strange that the T_m of PEG in sample 6 is higher than that in sample 8, which has the same T_m value as pure PEG, and that PEG in sample 6 has a much lower ΔH_f (2.4 J/g) than in sample 8 (20.3 J/g). Here it should be kept in mind that for sample 6 the PEG domain size may still be very small and most of the PEG chains are embedded in the silica networks. Hence, a small ΔH_f value means low crystallinity and an increased T_m value implies that some constrictions are also imposed on the PEG crystallites.[10]

Table II Thermal Data for PEG-TEOS Hybrid Materials

Sample No.	T_g (K)	T_m (K)	ΔH_f (J/g)[a]	T_{cr} (K)	ΔH_{cr} (J/g)[a]
2	374				
3	369				
6	361	327.6	2.4	304.3	11.3
8	357	323.6	20.3	300.3	25.8

[a] The values are normalized.

^{13}C and ^{29}Si Solid State NMR

The DSC results can be reasonably explained by ^{13}C- and ^{29}Si-NMR results on a molecular level. Shown in Figure 3 are the solid-state ^{29}Si-NMR MAS spectra of selected samples 3, 4, 5, and 8. Based on the peak assignments from model compounds,[11–13] three states of Si coordination about SiO_4 tetrahedra (Q^2, Q^3, and Q^4) are found with $Q^3 = (SiO)_3Si(OR)$ in the greatest abundance.

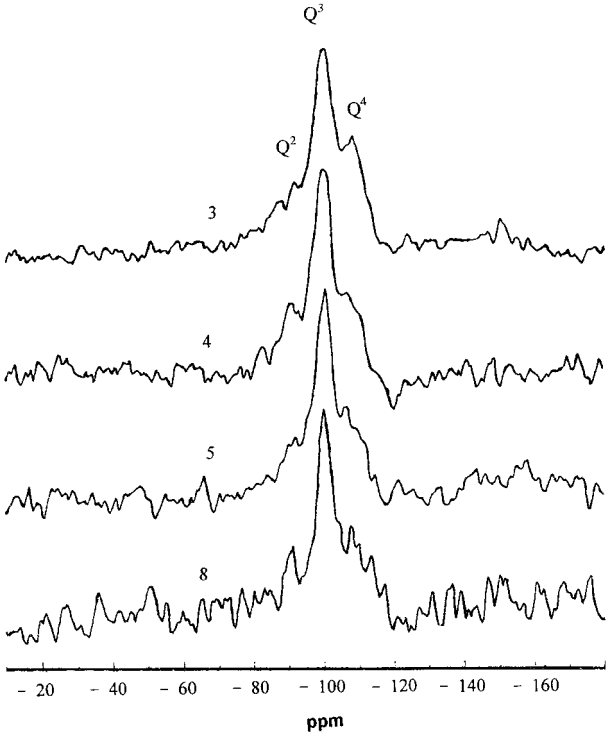

Figure 3 ^{29}Si MAS NMR spectra of samples 3, 4, 5, and 8.

More SiO_4 groups are tetra- than disubstituted. No Q^1 or TEOS peak appears. At the same time, it is clear that the existence of PEG chains has a considerable effect on the microstructure of the silica network. With the increase in PEG content, the relative content of Q^4 decreases and the content of Q^2 increases. This means that an increase of silica network defects, which results from the increased PEG content, in turn gives rise to effects on the morphology of PEG in the hybrids. ^{13}C-NMR spectra, shown in Figure 4, give more important information about the microstructure of the silica network. Figure 4 clearly shows that the intensity of the methyl resonance peak at 18.0 ppm, which represents the quantity of the Si-ethoxyl group, is much smaller than that of the PEG resonance peak around 70.0 ppm. It should be kept in mind that each Q^3 has one OR group (R = H or CH_2CH_3), and each Q^2 contains two OR groups. The much smaller intensity of the methyl peak indicates that the hydrolysis is nearly complete, and the hybrids contain great quantities of silanols. Roughly estimated, the mole ratio of silanols to PEG-OH is 300 for sample 2 and 20 for sample 8. This means that there are enough silanols for the formation of PEG—C—O—Si covalent and/or PEG—OH$\cdot\cdot$OH—Si— hydrogen bonds, if they could really form. Our results do not support the above hypothesis; at least no evidence showed that the covalent and/or the hydrogen bonds do exist. In fact, ^{29}Si-NMR spectra indicate that, with the increase in PEG content, Q^2 content increases at the expense of Q^4 content.

The influence of PEG on the microstructure of the silica network may originate from two main sources. The first is that some PEG—C—O—Si covalents and/or PEG—OH$\cdot\cdot$OH—Si— hydrogen bonds form, which will, to different degrees, defer the condensation of silanols. Without doubt, this situation is favorable for the formation of homogeneous hybrids. The second source is that the existence of PEG chains dilutes the concentration of silanols and reduces the probability that silanols meet, which is the prerequisite for the condensation of silanols. Thus, many free silanols remain in the hybrids (i.e., the Q^4 content decreases and the Q^2 and Q^3 contents correspondingly increase). In this work, we think the latter is dominant, otherwise we cannot explain the fact that phase separation becomes worse with the increase in PEG content. A very important conclusion drawn from the ^{13}C- and ^{29}Si-NMR spectra is that the lower the PEG content in the hybrids, the

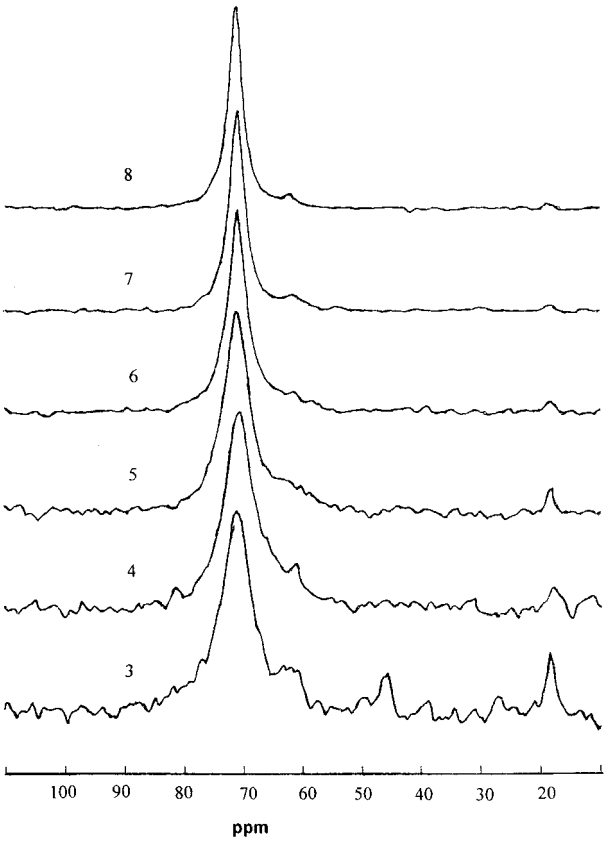

Figure 4 ^{13}C CPMAS NMR spectra for samples 3–8.

Table III ^{13}C Spin-Lattice Relaxation Times T_1 (C)(s) of PEG Hybrid Materials

Sample No.	T_1 (C)	Percent	T_1 (C)	Percent
3			2.5	100
4	0.3	42	2.6	58
5	0.3	65	2.7	35
6	0.3	70	3.0	30
7	0.2	70	2.7	30
8	0.2	69	3.0	31

Estimated error $\leq \pm 10\%$.

more perfect the silica network. It is significant for us to understand the fact that the lower the PEG content, the higher the T_g of PEG in the hybrids.

Nuclear Spin Relaxation

DSC and ^{29}Si-NMR results imply that the microstructure and mobility of PEG in hybrid materials changes a lot. As a powerful tool for characterizing microstructure and mobility of polymers, nuclear spin relaxation should offer more detailed information about them. As is well known, ^{13}C spin-lattice relaxation time, $T_1(C)$, can give the information about the motion of main-chain carbons on a megahertz regime.[14] Usually rigid chains will have a longer $T_1(C)$ value than mobile ones. The $T_1(C)$ values of PEG in hybrids, listed in Table III, clearly show that $T_1(C)$ values change with the PEG content. When the PEG content is low (sample 3), a single longer $T_1(C)$ value can be observed, indicating that some restrictions are imposed on the PEG chains. A single longer $T_1(C)$ value for sample 3 is in accordance with the DSC evidence of noncrystalline PEG with much higher T_g in this sample. As the PEG content increases, two $T_1(C)$ values occur. Except for the longer $T_1(C)$ value belonging to the restricted chains, a shorter $T_1(C)$ appears, which can be ascribed to the relaxation from the region rich in PEG. Another point worthy of mention is that the relative content of the PEG rich phase increases with PEG content in the hybrids because the relative content of the shorter $T_1(C)$ component increases correspondingly. Its consequence is that the domain size of the PEG rich phase becomes larger and larger and finally crystallites form within these domains. More direct evidence for the increase of mobile PEG chains with increased PEG content is that the line width at half-height of the ^{13}C spectra dramatically decreases from the 574 Hz of sample 3 to the 287 Hz of samples 7 and 8 (see Fig. 4, Table IV). From Figure 4 and Table IV we can find that a maximum PEG content exists, in this case say 50 wt %, beyond which a further increase in PEG content has almost no effect on the ^{13}C line width, implying that in this case the domain size of the PEG rich phase is so big that the PEG chains do not "feel" the existence of the silica network; in other words, the PEG chains in the rich phase have the same freedom as pure PEG chains. Therefore, they should exhibit the same crystallization behavior as that of pure PEG chains. This result is in excellent agreement with that from DSC. The results from proton spin–spin relaxation times, $T_2(H)$ further support this conclusion.

Other NMR Measurements

Until now we have had no idea about the homogeneity of hybrid materials. As is well known, proton spin-lattice relaxation in a rotating frame, $T_{1\rho}(H)$, is a very useful parameter for characterizing the homogeneity of multicomponent systems. A single $T_{1\rho}(H)$ value was used as a criterion for the miscibility or homogeneity of multicomponent polymer systems.[15–17] Shown in Figure 5 are the plots of logarithmic ^{13}C resonance intensity vs. proton spin-locking time for pure PEG and its hybrids, and the corresponding $T_{1\rho}(H)$ values are listed in Table V. For pure PEG, two $T_{1\rho}(H)$ values are observed. This result agrees with the fact that PEG is a semicrystalline polymer. When PEG chains are incorporated into the silica network, quite different situations occur. For hybrids with PEG content less than 30% by weight (samples 2 and 3), a single $T_{1\rho}(H)$ value is observed. This means that spin diffusion[18] via strong proton dipolar coupling is efficient enough to damp out nonequilibrium magnetization in any part of the proton spin systems in samples 2 and 3. The maximum displace L resulting from spin diffusion during a time t can be calculated by the equation[19]

$$L = \sqrt{6Dt} \qquad (1)$$

Table IV Line Width at Half-Height (Δ_L) of ^{13}C CPMAS NMR Spectra for Hybrid Materials

	Sample No.					
	3	4	5	6	7	8
Δ_L (Hz)	574	517	488	344	287	287

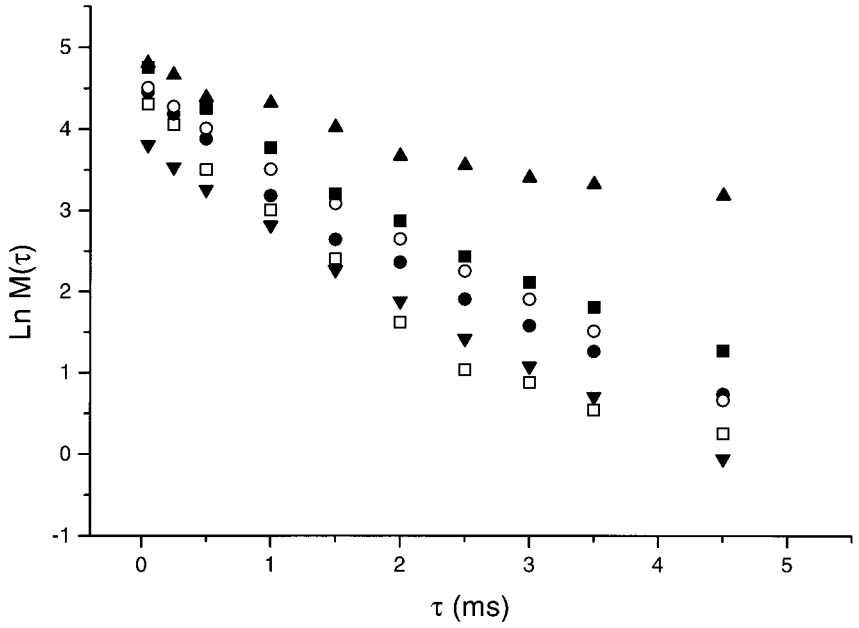

Figure 5 Plots of logarithmic ^{13}C resonance intensity vs. proton spin-locking time for samples: (▲) pure PEG, (▼) sample 3, (□) sample 4, (●) sample 6, (○) sample 7, and (■) sample 8.

where D is the diffusion coefficient taking an average value of $D = 5 \times 10^{-12}$ cm^2/s for polymers.[19] For a $T_{1\rho}$(H) value of 1 ms, considering that spin diffusion in the rotating frame is scaled by a factor of $\frac{1}{2}$, we can immediately estimate that the limiting size of the PEG domain in samples 2 and 3 is on the order of about 10–20 Å. Obviously, PEG chains in samples 2 and 3 are homogeneously dispersed within the silica network. As for samples 4–8, an obvious biexponential decay is observed. Phase separation undoubtedly occurs in these samples.

Interestingly, a clearer microstructure can be obtained from proton spin–spin relaxation time, T_2(H). Figure 6 shows the curves of T_2(H) decay of hybrids with different PEG content, and corresponding T_2(H) values are listed in Table VI. Figure 6 clearly shows that for molecular dispersion of PEG (samples 2 and 3), biexponential decay can be observed. One component has a much shorter T_2(H) value, indicating that the PEG chains in this case are rigid; and the other component has a much longer T_2(H), which is almost close to the T_2(H) of the PEG rich phase in sample 8, although its relative content is only around 20%. Here it should be kept in mind that the PEG chains are uniformly dispersed within the silica network in this case. Hence, the existence of biexponential components suggests that the silica network is not uniform, and defects or looser networks exist in the hybrids. This conclusion is in accordance with the ^{29}Si-NMR results. PEG chains may take the mode of an extended chain going through the silica network. The PEG segments within the tighter or more perfect silica network show a much shorter T_2(H), and the PEG segments on the looser silica network or network defects will have a longer T_2(H). Even if the PEG segments locate on the network defects, their T_2(H) is also shorter than that of crystalline PEG, indicating that there are some constrictions imposed on the PEG segments. The extended-chain behavior of PEG in silica networks is helpful to understand why the T_g of PEG in silica net-

Table V $T_{1\rho}$ (H) Values (ms) of PEG and PEG-TEOS Hybrid Materials

Sample No.	$T_{1\rho}$ (H)	Percent	$T_{1\rho}$ (H)	Percent
1	1.2	81.5	6.3	18.5
3	1.1	100		
4	0.2	41.2	0.8	58.8
5	0.2	42.8	0.9	57.2
6	0.5	55.0	1.3	45.0
7	0.5	36.1	1.3	63.9
8	0.6	54.5	1.4	45.5

Estimated error $\leq \pm 10\%$.

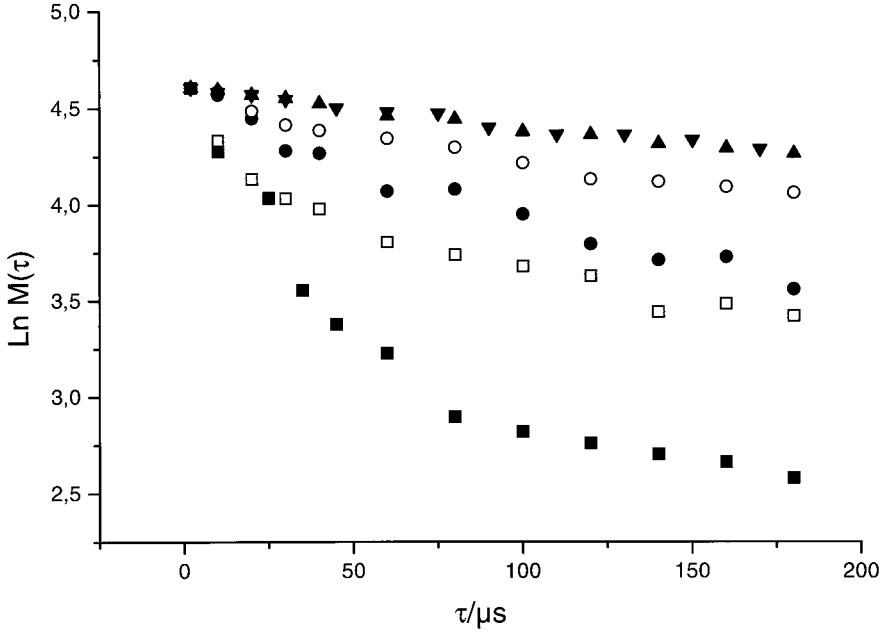

Figure 6 Plots of proton spin–spin relaxation for samples: (■) sample 3, (□) sample 4, (●) sample 5, (○) sample 6, (▲) sample 7, and (▼) sample 8.

works is much higher than that of pure PEG and even much higher than the T_m of PEG crystallites, and why the lower the PEG content in heterogeneous hybrids, the higher the T_m of PEG crystallites, if they exist. As the PEG content increases, the relative content of the shorter T_2(H) component decreases. Meanwhile, the shorter T_2(H) value becomes slightly longer, indicating fewer restrictions on the PEG chains (i.e., the silica network becomes less perfect with the increase in PEG content). This result is in agreement with the increase in Q^2 content at the expense of a decrease in Q^4 content and the decrease of T_g of PEG in hybrids as PEG content increases. A further increase in PEG content makes the longer T_2(H) component become dominant. Finally, for samples 7 and 8 the content of the shorter T_2(H) component becomes so small that only a single longer T_2(H) can be detected. In this case, the crystallization behavior of PEG in the hybrids is similar to that of pure PEG. As pointed out above, when PEG content is beyond some range, in this case 50% by weight, a further increase in PEG content has no effect on T_2(H) value, indicating that the domain size of the phase separation is so big that PEG chains exhibit properties similar to that of bulk PEG. One of its macroscopic consequences is that the T_m of PEG crystallites in hybrids is the same as that of pure PEG.

Table VI T_2 (H) Values (μs) of PEG-TEOS Hybrid Materials

Sample No.	T_2 (H)	Percent	T_2 (H)	Percent
3	19	77	271	23
4	26	51	262	49
5	35	36	283	64
6	33	19	467	81
7			498	100
8			513	100

Estimated error $\leq \pm 5\%$.

CONCLUSIONS

By a combination of the results from DSC and ^{13}C- and ^{29}Si-NMR, we can draw the following conclusions: The microstructure of PEG-TEOS hybrid materials strongly depends on their compositions. Truly homogeneous PEG-TEOS hybrids can be obtained via a sol–gel process provided the PEG content is lower than, say 30% by weight. The presence of PEG has a considerable effect on the microstructure of the silica network, which in turn influences the morphology of PEG. The effect of PEG on the microstructure of the silica network mainly results from the diluting and separating effects of PEG chains on silanols. With increasing PEG content, the morphology and mobility of PEG changes a lot, from uniform dispersion on a molec-

ular level to microphase separation, and finally to macrophase separation. In homogeneous hybrids PEG segments, taking the mode of an extended chain, have a T_g 150 K higher than that of pure PEG. In macrophase separation systems, the crystallization behavior of PEG is quite similar to that of pure PEG.

The authors are grateful for the financial support granted by the National Natural Science Foundation of China and the Laboratory of Magnetic Resonance and Atomic and Molecular Physics, Wuhan Institute of Physics and Mathematics, Chinese Academy of Sciences.

REFERENCES

1. B. M. Novak, *Adv. Mater.,* **5,** 42 (1993).
2. H.-H. Huang, B. Orler, and G. L. Wilkes, *Macromolecules,* **20,** 1322 (1987).
3. H.-H. Huang and G. L. Wilkes, *Polym. Bull.,* **18,** 455 (1987).
4. H. Schmidt, *J. Non-Cryst. Solids,* **112,** 419 (1989).
5. D. Ravaine, A. Seminel, Y. Charbouillot, and M. Vincens, *J. Non-Cryst. Solids,* **82,** 210 (1986).
6. T. Saegusa, *J. Macromol. Sci. Chem. A,* **28,** 817 (1991).
7. D. A. Torchia, *J. Magn. Reson.,* **30,** 613 (1978).
8. A. J. Nijenhuis, E. Colstee, D. W. Grijpma, and A. J. Pennings, *Polymer,* **37,** 5849 (1996).
9. G. V. Schulz, H. Hässlin, and M. Dröscher, *Makromol. Chem.,* **181,** 2375 (1980).
10. D. C. Bassett, *Principles of Polymer Morphology,* Cambridge University Press, New York, 1981.
11. W. G. Klimperer and S. D. Ramamurthi, *Polym. Prepr. (ACS)* **28,** 432 (1987).
12. R. J. Hook, *J. Non-Cryst. Solids,* **1,** 195 (1996).
13. H. Eckert, *Prog. NMR Spectrosc.,* **24,** 159 (1992).
14. J. Schaefer, E. O. Stejskal, and R. Buchdahl, *Macromolecules,* **10,** 384 (1976).
15. E. O. Stejskal, J. Schafer, M. D. Sefcik, and R. A. Mckey, *Macromolecules,* **14,** 275 (1981).
16. R. A. Komoroski, *High Resolution NMR Spectroscopy of Synthetic Polymers in Bulk,* VCH Publishers, Inc., New York, 1986.
17. H. Feng, J. Tian, and C. Ye, *J. Appl. Polym. Sci.,* **61,** 2265 (1996).
18. A. Abragam, *The Principles of Nuclear Magnetism,* Oxford University Press, London, 1961.
19. W. S. Veeman and W. E. J. R. Maas, *NMR Basic Principles Prog.,* **32,** 127 (1994).